WORLD CONFERENCE ON TIMBER ENGINEERING 2025
BRISBANE, AUSTRALIA

Advancing Timber for the Future Built Environment

EVALUATION OF CLT SEISMIC RESISTANT WALLS WITH ARBITRARILY ARRANGED GIR JOINTS

Daisuke Kadono[1], Shuhei Uesugi[2], Shunsuke Toyao[3], Tsubasa Seguchi[4], Katsuhide Murakami[5], Masahide Murakami[6]

ABSTRACT: GIR joints with steel bars are a relatively inexpensive method of joining high strength and rigidity to wood materials, and can be used to join CLT walls to surrounding framing to achieve high strength earthquake-resistant walls. In a previous report[1], cyclic loading test results of CLT walls with GIR joints were presented, showing that high bearing capacity and energy absorption can be obtained and that the performance under cyclic loading can be predicted by numerical calculations. In this paper, an evaluation formula is proposed to estimate the stiffness and bearing capacity at the wall footings for an arbitrary GIR joint arrangement by hand calculations, and the results are compared with previous experimental results. In past experiments, GIR joints close to the surface of the CLT sometimes failed to exhibit the expected bearing capacity because of crack failure when large tensile forces due to rotation of the wall footings were applied to the GIR joints. We have developed a crack reinforcement method for GIR joints using steel tubes and wood screws, with which the CLT wall can exhibit the designed bearing capacity and toughness.

KEYWORDS: CLT, CLT wall, GIR joints, Evaluation formula, Crack Reinforcement

1 – INTRODUCTION

In Japan, where high earthquake resistance is required for buildings, CLT, a wood material with high rigidity and strength, is increasingly being used as an earthquake-resistant element in steel frame and reinforced concrete structures as well as in wooden structures. We have been developing CLT seismic resistant walls using GIR joints, which can achieve high strength and stiffness with relatively inexpensive materials (shown in Fig. 1). In this paper we report

- Evaluation formulas to estimate separation, yield, and ultimate capacity of CLT seismic walls.
- Crack reinforcement method for GIR joints subjected to tensile forces using steel tubes and long screws.

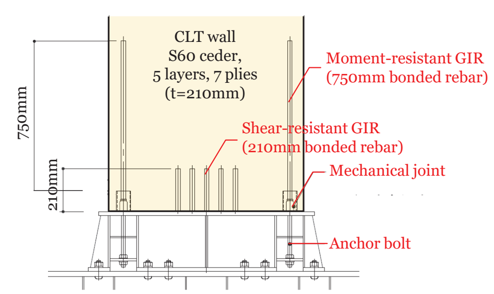

Figure 1 The footing of CLT seismic wall in this report

2 – BACKGROUND

In a previous report[1], we conducted cyclic loading tests on CLT seismic walls. We then compared the results using an analytical model with multi-springs in the wall footings and found good agreement. It was confirmed that the moment capacity of the wall footings increased due to axial force introduced into the walls. If we can model the rotation mechanism of the CLT wall footings and derive an evaluation formula that takes axial forces into account, we can quickly calculate the performance of CLT walls without numerical analysis and clarify the

[1] Daisuke Kadono, NIKKEN SEKKEI LTD, Japan, kadono.daisuke@nikken.jp

[2] Shuhei Uesugi, NIKKEN SEKKEI LTD, Japan, uesugi.shuhei@nikken.jp

[3] Shunsuke Toyao, NIKKEN SEKKEI LTD, Japan, toyao.shunsuke@nikken.jp

[4] Tsubasa Seguchi, NIKKEN SEKKEI LTD, Japan, seguchi.tsubasa@nikken.jp

[5] Katsuhide Murakami, NIKKEN SEKKEI LTD, Japan, murakamik@nikken.jp

[6] Masahide Murakami, Former Prof., Dept of Architecture, Faculty of Architecture, KINDAI University, Japan, Dr.Eng. murakami@arch.kindai.ac.jp

https://doi.org/10.52202/080513-0133

mechanism of the increase of moment capacity due to axial force at the wall footings.

Inayama[2] and Akiyama[3] have previously researched on the glulam frame structure with tensile-bolted moment resisting joints, and proposed a calculation method of the stiffness and strength of column-base joints subject to axial force. The CLT seismic wall subjected to this paper has a similar mechanism to the tensile-bolted moment resisting joint in that it resists bending by means of an axial resisting element and the bearing pressure of the wood members. On the other hand, the GIR joints are expected to resist not only tension but also compression, and the fact that multiple joint elements, including the GIR joints placed in the center, contribute to the bending stiffness and bearing capacity, are unique to the CLT wall in this report, and a new evaluation method is needed.

In the course of loading tests of CLT seismic walls, crack failure has frequently occurred at the GIR joints close to the CLT surface, causing the CLT walls to lose their bearing capacity before the CLT seismic walls are fully deformed. Preventing crack failure at the moment-resistant GIR joints of the wall footings when the wall footings rotate is important to ensure the toughness of the wall as an seismic resistant wall, and a method of reinforcing GIR joints embedded in wood members against cracks is needed.

3 – LOAD-BEARING MECHANISM AND CAPACITY EVALUATION FORMULAS

Based on the balance of axial forces and moments in the CLT wall footing, the angle of rotation of the wall footing, the position of the neutral axis, and the wall footing moment are obtained for the following conditions: (I) when the end of the wall footing is separated, (II) when the end of the wall footing yields, and (III) when the ultimate bearing capacity is reached.

3.1 ASSUMPTIONS AND PARAMETERS

The rotation mechanism of the wall footing subjected to horizontal forces is shown in Fig. 2. The lifting and sinking of the wall footings are assumed to be linearly distributed. Based on this assumption, the amount of lift and sinkage at each position of the wall footing is uniquely determined by the rotation angle θ of the wall footing and the neutral axis position x_n. The GIR position on the wall footing is equipped with an axial spring corresponding to the GIR diameter and anchorage length. The GIR arrangement is arbitrary. In the region on the compression side of the CLT above the neutral axis, a plane bearing spring is considered because of the expected bearing resistance between the CLT and the foundation. The sign of each parameter value is also shown in Fig. 2.

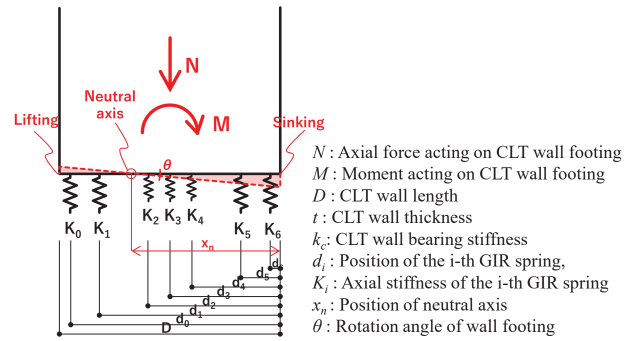

Figure 2 Rotation mechanism of wall footing and parameters

3.2 DERIVATION OF SEPARATION CAPACITY

The wall footing moments are obtained for the condition shown in Fig. 3, where the wall footings are separated at the outermost GIR position. Substitute (3) for the compressive force due to the bearing pressure of the CLT wall footing and (4) for the GIR axial force at each position into (1) and (2), which show the balance between axial force and moment, to obtain the rotation angle θ_0 at separation and the separation-resistant moment M_0 as in (5) and (6).

$$N = C + \sum C_i \tag{1}$$

$$M = C(D/2 - d_0/3) + \sum \{C_i(D/2 - d_i)\} \tag{2}$$

$$C = k_c t {d_0}^2 \theta_0 / 2 \tag{3}$$

$$C_i = K_i(d_0 - d_i)\theta_0 \tag{4}$$

$$\theta_0 = N / \left[k_c t {d_0}^2/2 + \sum \{K_i(d_0 - d_i)\}\right] \tag{5}$$

$$M_0 = \left[\frac{1}{2} k_c t {d_0}^2 \left(\frac{D}{2} - \frac{d_0}{3}\right) + \sum \left\{K_i(d_0 - d_i)\left(\frac{D}{2} - d_i\right)\right\}\right] \cdot \theta_0 \tag{6}$$

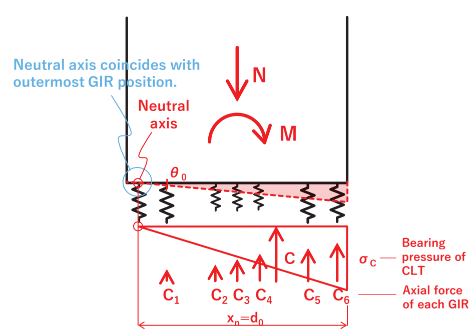

Figure 3 Assumptions when separation capacity is reached

https://doi.org/10.52202/080513-0133

3.3 DERIVATION OF YIELD CAPACITY

Three cases (i) through (iii) are assumed depending on the neutral axis position x_n shown in Fig. 4. Two values are obtained, one is the wall footing moment M_{yc} at which the compressive edge bearing stress σ_c reaches the CLT bearing strength fc, and the other is M_{yt} at which the outermost GIR axial force reaches the yield capacity T_y. For each case, (7) and (8), which show the balance of axial forces and moments, are substituted for (9) and (10), which show the bearing pressure and GIR axial force, and for (11) and (14), which show the rotation angle at which M_{yc} and M_{yt} are reached. Then, the solution(12) and (15) for the neutral axis position x_n is obtained, and M_{yc}, M_{yt} are obtained as in (13),(16). In case(ii), the smaller of M_{yc} and M_{yt} is taken as the yield capacity.

Case(i):

$$N - C - \sum C_i = 0 \tag{7i}$$

$$M = C \cdot \frac{D}{6}\left(\frac{2x_n}{D} - 1\right)^{-1} + \sum\{C_i(D/2 - d_i)\} \tag{8i}$$

$$C = k_c t D(2x_n - D)\theta/2 \tag{9i}$$

$$C_i = K_i(x_n - d_i)\theta \tag{10i}$$

$$\theta_c = f_c/k_c x_n \tag{11i}$$

$$x_n = \left(2D + n_e \sum \frac{K_i d_i}{K_0}\right) \Big/ \left(4 - \frac{N}{C_{ne}} + n_e \sum \frac{K_i}{K_0}\right) \tag{12i}$$

$$M_{yc} = 2C_{ne}\left(2 - \frac{D}{x_n}\right)\frac{D}{6}\left(\frac{2x_n}{D} - 1\right)^{-1} + n_e C_{ne}\frac{1}{x_n}\sum\left\{\frac{K_i}{K_0}(x_n - d_i)\left(\frac{D}{2} - d_i\right)\right\} \tag{13i}$$

Case(ii):

$$N - C + \sum T_i - \sum C_i = 0 \tag{7ii}$$

$$M = C(D/2 - x_n/3) + \sum\{T_i(d_i - D/2)\} + \sum\{C_i(D/2 - d_i)\} \tag{8ii}$$

$$C = k_c t x_n^2 \theta/2 \tag{9ii}$$

$$T_i = -C_i = K_i(d_i - x_n)\theta \tag{10ii}$$

$$\theta_c = f_c/k_c x_n \tag{11ii}$$

$$x_n = \frac{n_e D}{4}\left\{\frac{N}{n_e C_{ne}} - \sum\frac{K_i}{K_0} + \sqrt{\left(\frac{N}{n_e C_{ne}} - \sum\frac{K_i}{K_0}\right)^2 + \frac{4}{n_e D}\cdot 2d_0 \sum\frac{K_i d_i}{K_0 d_0}}\right\} \tag{12ii}$$

$$M_{yc} = \frac{f_c t \cdot n_e D}{4x_n}\left[\frac{2x_n^2}{n_e D}(D/2 - x_n/3) + \sum\left\{\frac{K_i}{K_0}(d_i - x_n)(d_i - D/2)\right\}\right] \tag{13ii}$$

$$\theta_y = T_y/K_0(d_0 - x_n) \tag{14ii}$$

$$x_n = \frac{n_e D}{4}\left\{-\left(\frac{N}{T_y} + \sum\frac{K_i}{K_0}\right) + \sqrt{\left(\frac{N}{T_y} + \sum\frac{K_i}{K_0}\right)^2 + \frac{4}{n_e D}\cdot 2d_0\left(\frac{N}{T_y} + \sum\frac{K_i d_i}{K_0 d_0}\right)}\right\} \tag{15ii}$$

$$M_{yt} = T_y/(d_0 - x_n)\left[\frac{2}{n_e D}x_n^2(D/2 - x_n/3) + \sum\left\{\frac{K_i}{K_0}(d_i - x_n)(d_i - D/2)\right\}\right] \tag{16ii}$$

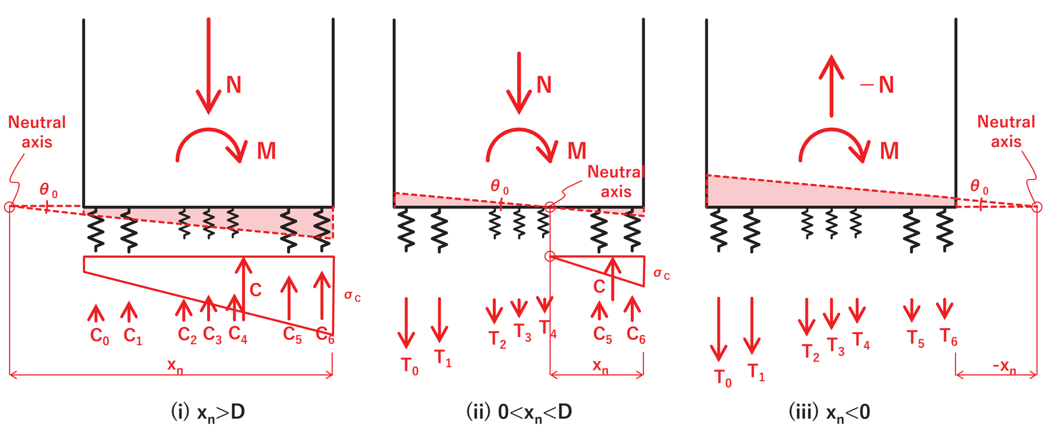

Figure 4 Assumptions when yield capacity is reached

https://doi.org/10.52202/080513-0133

Case(iii)：

$$N + \sum T_i = 0 \qquad (7iii)$$

$$M = \sum \{T_i(d_i - D/2)\} \qquad (8iii)$$

$$T_i = K_i(d_i - x_n)\theta \qquad (9iii)$$

$$\theta_y = T_y / K_0(d_0 - x_n) \qquad (14iii)$$

$$x_n = d_0 \cdot \left(\frac{N}{T_y} + \sum \frac{K_i d_i}{K_0 d_0}\right) \Big/ \left(\frac{N}{T_y} + \sum \frac{K_i}{K_0}\right) \qquad (15iii)$$

$$M_{yt} = {}^{T_y}\!\Big/_{(d_0 - x_n)} \sum \left\{\frac{K_i}{K_0}(d_i - x_n)(d_i - {}^{D}\!/_{2})\right\} \qquad (16iii)$$

Common：n_e and C_e are according to following.

$$n_e = 4K_0 / k_c t D \qquad (17)$$

$$C_{ne} = f_c t D / 4 \qquad (18)$$

3.4 DERIVATION OF ULTIMATE CAPACITY

In evaluating the ultimate bearing capacity, the three cases shown in Fig. 5 are assumed according to the magnitude of axial force N. The i-th GIR tensile bearing capacity is Tui and the i-th GIR compressive bearing capacity is Cui. In the range of axial forces actually used, many cases are considered to correspond to (II), and the derivation of the ultimate bearing capacity equation in (II) is presented here. From the balance of the forces,

$$N - F_c t x_n + \sum_{\square}^{left} T_{ui} - \sum_{\square}^{right} C_{ui} = 0 \qquad (19)$$

Solving (19) for x_n, the length of pressured range on the wall footing, we obtain

$$x_n = \left(N + \sum_{\square}^{left} T_{ui} - \sum_{\square}^{right} C_{ui}\right) \Big/ F_c t \qquad (20)$$

On the other hand, from the balance of the moments,

$$M_u = F_c t x_n ({}^{D}\!/_{2} - {}^{x_n}\!/_{2})$$
$$+ \sum_{\square}^{left} T_{ui}(d_i - {}^{D}\!/_{2}) + \sum_{\square}^{right} C_{ui}({}^{D}\!/_{2} - d_i) \qquad (21)$$

Substituting the solution of x_n by (20) into (21), the ultimate moment M_u is obtained.

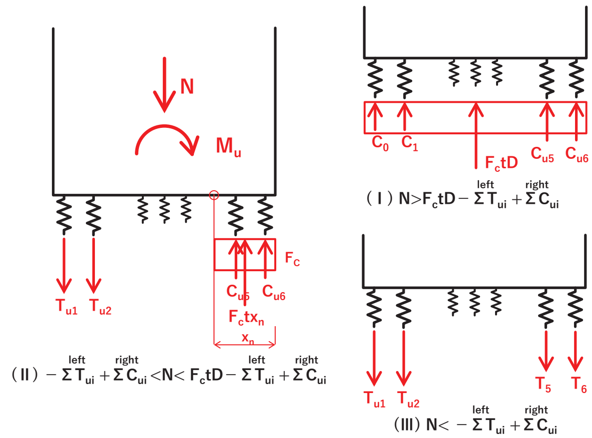

Figure 5 Assumptions when ultimate capacity reached

Next, as shown in Fig. 6, the point at which the elongation of the outermost end GIR reaches εl_b is considered to be the final deformation state. where ε is the maximum elongation rate and l_b is the elongation length of the outermost GIR connecting bolt. From the relationship between the elongation of the outermost GIR and the angle of rotation, we obtain

$$(d_0 - x_n)\theta_u = \varepsilon l_b \qquad (22)$$

Solving the above equation for the final rotation angle θ_u yields

$$\theta_u = \varepsilon l_b / (d_0 - x_n) \qquad (23)$$

Substituting the solution (20) for the neutral axis position x_n when the ultimate bearing capacity is reached into (23), the ultimate rotation angle θ_u is obtained.

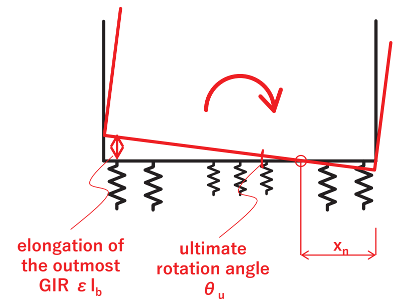

Figure 6 Assumptions when ultimate deformation reached

3.5 DERIVATION OF HISTORY CURVE

A bilinear type history curve is obtained by connecting the calculated values of separation, yield, and ultimate bearing capacity. Fig. 7 compares the result from loading tests conducted to date on 16 CLT seismic walls

https://doi.org/10.52202/080513-0133

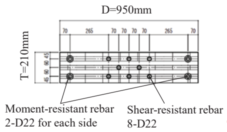

Axial Force: N=268kN(Compression)
Property of CLT:
kc=27.3N/mm^3, fc=25.1N/mm^2,
Fc=25.1N/mm^2 ,G=500N/mm^2
Property of each Moment-resistant rebar:
Kt=127kN/mm, Ty=141kN, Tu=201kN,
Cu=131kN
Property of each Shear-resistant rebar:
Kt=11.1kN/mm(embedded in 2nd & 6th layer),
12.9kN/mm(embedded in 4th layer)
Ks=35kN/mm

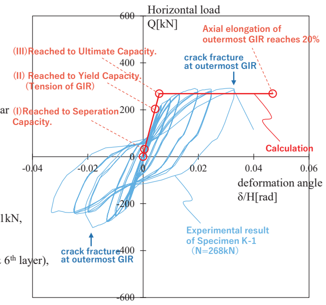

(i) Specimen K-1

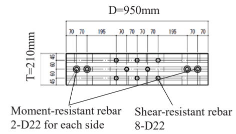

Axial Force: N=268kN(Compression)
Property of CLT:
kc=27.3N/mm^3, fc=25.1N/mm^2,
Fc=25.1N/mm^2 ,G=500N/mm^2
Property of each Moment-resistant rebar:
Kt=90kN/mm, Ty=141kN, Tu=201kN,
Cu=131kN
Property of each Shear-resistant rebar:
Kt=11.1kN/mm(embedded in 2nd & 6th layer),
12.9kN/mm(embedded in 4th layer)
Ks=35kN/mm

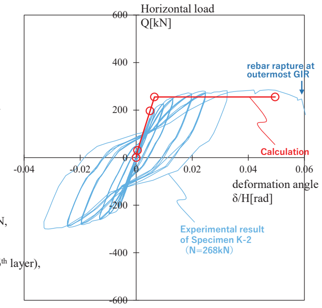

(ii) Specimen K-2

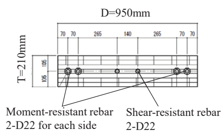

Axial Force: N=268kN(Compression)
Property of CLT:
kc=27.3N/mm^3, fc=25.1N/mm^2,
Fc=25.1N/mm^2 ,G=500N/mm^2
Property of each Moment-resistant rebar:
Kt=90kN/mm, Ty=141kN, Tu=201kN,
Cu=131kN
Property of each Shear-resistant rebar:
Kt=12.9kN/mm(embedded in 4th layer)
Ks=35kN/mm

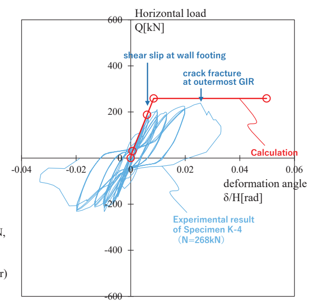

(iii) Specimen K-4

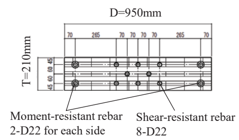

Axial Force: N=0kN
Property of CLT:
kc=27.3N/mm^3, fc=25.1N/mm^2,
Fc=25.1N/mm^2 ,G=500N/mm^2
Property of each Moment-resistant rebar:
Kt=122kN/mm, Ty=141kN, Tu=201kN,
Cu=131kN
Property of each Shear-resistant rebar:
Kt=22.9kN/mm(embedded in 2nd & 6th layer),
26.1kN/mm(embedded in 4th layer)
Ks=35kN/mm

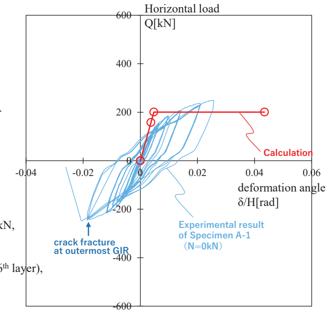

(iv) Specimen A-1

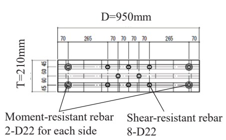

Axial Force: N=0kN
Property of CLT:
kc=27.3N/mm^3, fc=25.1N/mm^2,
Fc=25.1N/mm^2 ,G=500N/mm^2
Property of each Moment-resistant rebar:
Kt=122kN/mm, Ty=141kN, Tu=201kN,
Cu=131kN
Property of each Shear-resistant rebar:
Kt=22.9kN/mm(embedded in 2nd & 6th layer),
26.1kN/mm(embedded in 4th layer)
Ks=35kN/mm

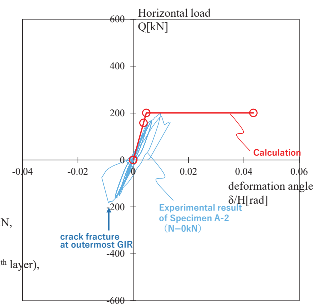

(v) Specimen A-2

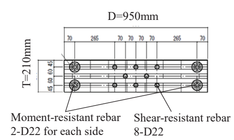

Axial Force: N=0kN
Property of CLT:
kc=27.3N/mm^3, fc=25.1N/mm^2,
Fc=25.1N/mm^2 ,G=500N/mm^2
Property of each Moment-resistant rebar:
Kt=219kN/mm, Ty=141kN, Tu=201kN,
Cu=131kN
Property of each Shear-resistant rebar:
Kt=22.9kN/mm(embedded in 2nd & 6th layer),
26.1kN/mm(embedded in 4th layer)
Ks=35kN/mm

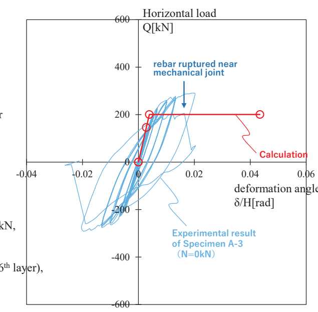

(vi) Specimen A-3

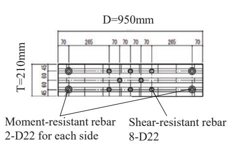

Axial Force: N=0kN
Property of CLT:
kc=27.3N/mm^3, fc=25.1N/mm^2,
Fc=25.1N/mm^2 ,G=500N/mm^2
Property of each Moment-resistant rebar:
Kt=122kN/mm, Ty=141kN, Tu=201kN,
Cu=131kN
Property of each Shear-resistant rebar:
Kt=22.9kN/mm(embedded in 2nd & 6th layer),
26.1kN/mm(embedded in 4th layer)
Ks=35kN/mm

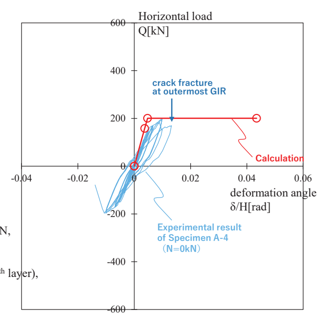

(vii) Specimen A-4

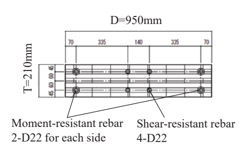

Axial Force: N=0kN
Property of CLT:
kc=27.3N/mm^3, fc=25.1N/mm^2,
Fc=25.1N/mm^2 ,G=500N/mm^2
Property of each Moment-resistant rebar:
Kt=129kN/mm, Ty=141kN, Tu=201kN,
Cu=131kN
Property of each Shear-resistant rebar:
Kt=22.9kN/mm(embedded in 2nd & 6th layer),
26.1kN/mm(embedded in 4th layer)
Ks=35kN/mm

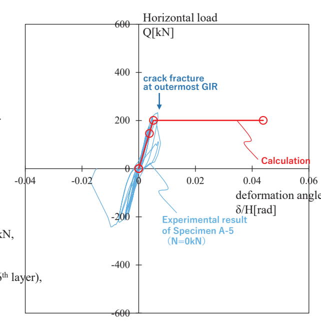

(viii) Specimen A-5

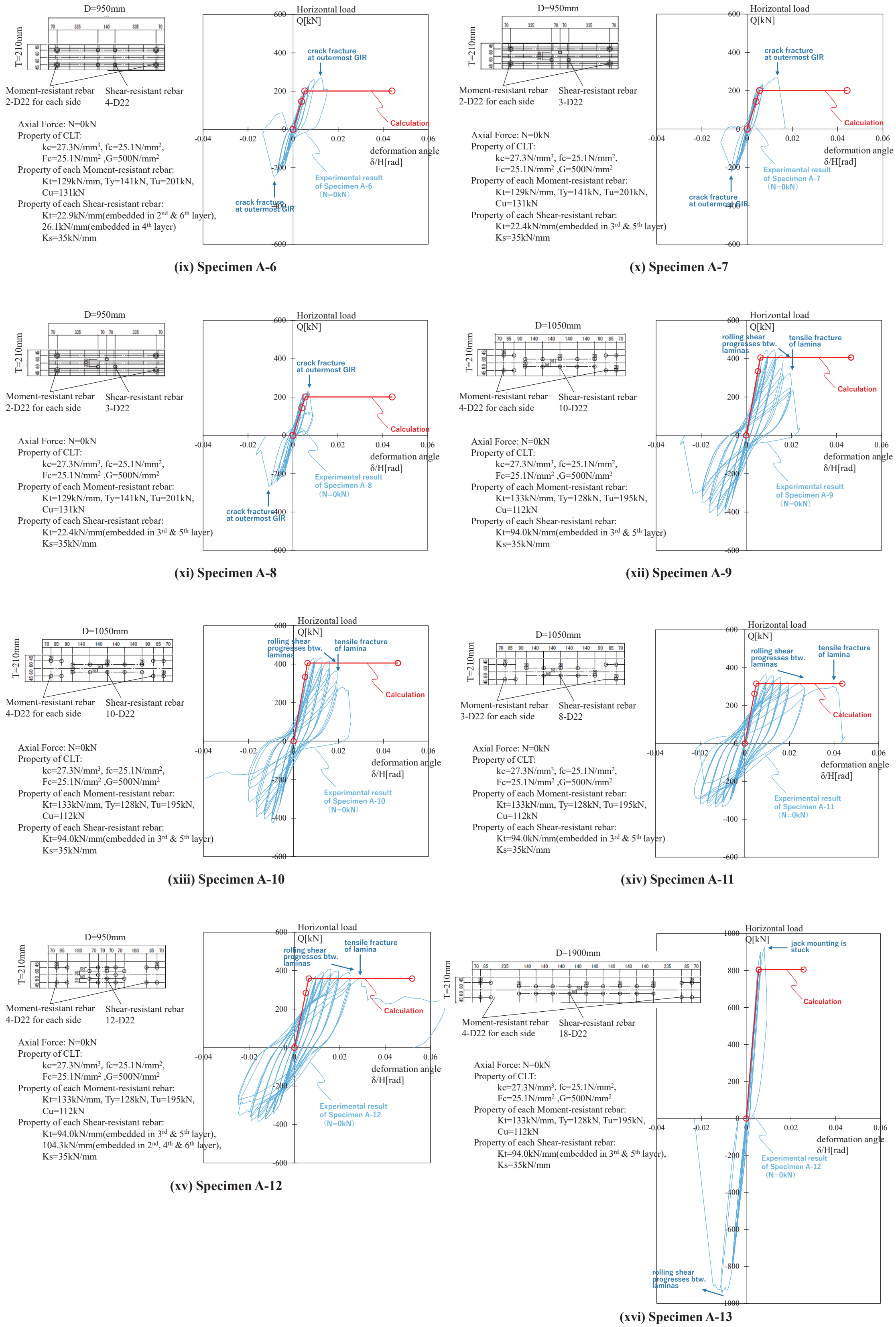

Figure 7 Comparison of the results of the CLT seismic wall tests and the history curves using the evaluation formula

https://doi.org/10.52202/080513-0133

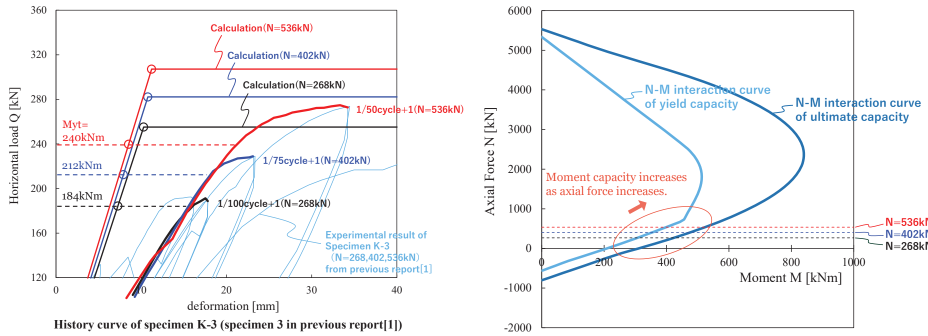

Figure 8 Increase in moment capacity due to axial force and N-M curve of yield and ultimate capacity

with the bilinear curves calculated using the evaluation formulas presented in this report. Calculation results show good estimation of trends in separation, yield, and ultimate capacity. In the K-2 specimen, where the outermost rebar eventually reached failure, the ultimate deformation angle of the wall was in general agreement with the calculated values. In the other specimens, the crack failure of the wood around the moment-resistant GIR and the failure of the CLT itself occurred before the rebar reached failure, resulting in a reduction in the bearing capacity.

3-6. Derivation of N-M bearing capacity curve

Using (13i), (13ii), (16ii), (16iii), and (21), the yield capacity and ultimate capacity under any axial force can be expressed as N-M interaction bearing capacity curve. For example, the N-M curve of specimen K-3 (Specimen 3 reported in a previous report[1], at which loading was performed while varying the introduced axial force) is given in Fig. 8. In the previous report, it was confirmed that the bending capacity increased when the magnitude of the introduced axial force was increased in steps from 268kN to 536kN, as shown in Fig. 8, and it can also be confirmed that the yield capacity and ultimate capacity increased on the N-M curve.

4 – DETAIL OF MOMENT-RESISTANT GIR AND CRACK REINFORCEMENT

It is important to prevent crack failure at the GIR joint of the moment-resistant GIR joints at the end of the wall footing when the wall footing rotates in order to ensure the toughness of the wall. We have confirmed that crack reinforcement using steel pipe rings and wood screws around D22 rebars anchored at the end of CLTs can reliably prevent cracking of the CLTs and precede the rupture of anchor bolts connected to the bars.

In the CLT wall subjected to this report, GIR joints are adopted, in which rebar D22 is buried 750 mm within the strong-axis layer (parallel to the fiber direction) in the CLT wall as a joint that resists the moment of the wall footing, and is bonded with the CLT by injecting adhesive. It was confirmed that the following specifications can reliably prevent brittle crack failure of the wood and precede the axial rupture of the anchor bolts connecting to the rebar. Fig. 9 shows the reinforcement method.

- Rebar D22 (SD345) is bonded 750 mm inside the CLT with epoxy adhesive and connected to ABR anchor bolt M27 via a mechanical joint.
- The shaft of the ABR anchor bolt M27 (SNR400 material) to be connected is pre-shaved 1.3 mm in diameter.
- Embed a ring of steel pipe (STKM13A material) with a diameter of 70mm and a thickness of 4.0 mm, cut into 100 mm long rings around the rebar at the end of the CLT.
- Drive two wood screws (6φ, all-thread type) in a diagonal direction near the beginning of the rebar anchorage.

The shaved dimensions of the ABR anchor bolts are set to provide approx. 90% of the axial capacity relative to the D22 deformed rebar. Tensile test results of GIRs with the above specifications are reported in previous reports [4][5], which are shown in Fig. 10. It was confirmed that the aforementioned crack reinforcement stably preceded the yielding and rupture of the anchor bolt shaft. Furthermore, it was also confirmed that similar properties were obtained when two rebars GIR were placed at a separation of 85 mm. By ensuring that tensile yielding and rupture are preceded on the anchor bolt side, stable energy absorption can be expected during wall footing rotational deformation. In addition, The anchor bolts connecting to the rebar have sufficient elongation sections outside the CLT. The anchor bolt ends are fastened with nuts from both sides of the anchorage PL, and the middle of the anchor bolt shaft is buckled with a horizontal plate to provide a mechanism that can resist not only tensile forces but also compressive forces.

https://doi.org/10.52202/080513-0133

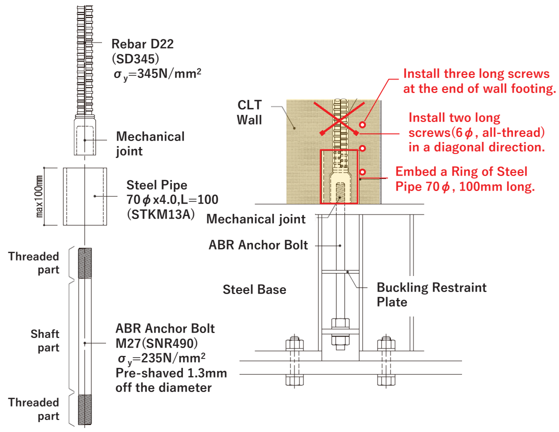

Figure 9 Detail of moment-resistant GIR joint with crack reinforcement

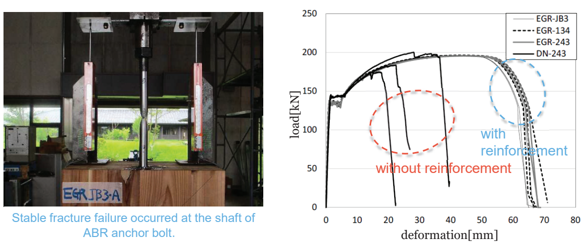

(i) Tensile test results of one-pull specimens

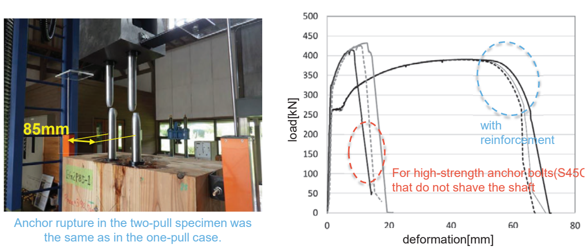

(ii) Tensile test results of two-pull specimens

Figure 10 Tensil joint test of GIR joints with crack reinforcement

5 – RESULTS AND CONCLUSIONS

The evaluation formulas for the rotation angle and moment capacity at the wall footing in the separation, yield, and ultimate states are derived for CLT seismic walls with GIR joints. The evaluation formulas are used to estimate the bearing capacities under any axial force for arbitrarily arranged GIR arrangement at the CLT wall footing.

The bilinear curves, which are derived using evaluation formulas in this report, was superimposed on the results of 16 CLT wall tests conducted to date, and it was confirmed that the separate capacity, yield capacity, and ultimate capacity of the CLT walls were in good agreement.

In some of the CLT wall loading tests, crack failure of the wood around the moment-resistant GIR joints occurred, causing a reduction in the bearing capacity of the CLT wall. In order to ensure the toughness of CLT seismic walls during earthquakes, it is necessary to avoid crack failure of the wood. For the CLT walls in this report, crack reinforcement using steel pipes and long screws was applied around the wall footing where the moment-resistant GIRs are embedded, and it was confirmed that the reinforcement was effective. In addition, by adjusting the diameter and strength of the connecting anchor bolts, it was possible to suppress the occurrence of crack failure and ensure that the anchor bolts' yielding was preceded.

6 – ACKNOWLEGEMENTS

The authors are grateful to Yamasa Mokuzai Col,Ltd., who contributed to making the test specimens and supported the experimental tests. Also grateful to Makoto Nakatani at Miyazaki Prefectural Forestry Technical Center, and to Kazuo Yonemoto at DAIROCK,LTD, who contributed to develop crack reinforcement method for GIR joints.

7 – REFERENCES

[1] S. Uesugi, D. Kadono, K. Murakami, and M. Murakami "Cyclic Load Tesing of a CLT Seismic Resistant Wall with GIR Joints" World Conference on Timber Engineering 2023 (in Japanese)

[2] Inayama,M.: Study on structural design method of timber semi-rigid columnbase joint drawn with tensile bolts, Summaries of Technical Papers of Annual Meeting, Architectural Institute of Japan, Structure III, pp.621-622, 2013.7 (in Japanese)

[3] Akiyama,N. et al.: Research on seismic design method for glulam frame structure with tensile-bolted moment resisting joints -Proposal for a design method to estimate stiffness and strength of column – base joints subject to axial force -, Journal of Structural and Construction Engineering, Vol.87, No.793, pp.295-306, 2022.3 (in Japanese)

[4] Nakatani,M. et al.: "*GIR oyobi LSB no katsuretsu-hakai ni taisuru hokyo houhou no kento*" [Research on reinforcement methods for crack failure of GIR and LSB], Journal of Timber Engineering, Vol.35, No.4, pp.159-164, 2022.12 (in Japanese)

[5] Murakami,K. et al.: "*Katsuretsu-hokyo wo hodokoshita kojinsei GIR setsugoubu no kaihatsu*" [Development of high-toughness GIR joints with crack reinforcement], Journal of Timber Engineering, Vol.38, No.3, 2023.9 (in Japanese)

https://doi.org/10.52202/080513-0133